SLAC-PUB-14391

# Two-dimensional Dirac fermions in a topological insulator: transport in the quantum limit

J.G. Analytis,[1,2] R.D. McDonald,[3] S. C. Riggs,[4] J.-H. Chu,[1,2] G. S. Boebinger,[4] and I.R. Fisher[1,2]

[1]*Stanford Institute for Materials and Energy Sciences, SLAC National Accelerator Laboratory, 2575 Sand Hill Road, Menlo Park, CA 94025, USA*

[2]*Geballe Laboratory for Advanced Materials and Department of Applied Physics, Stanford University, USA*

[3]*Los Alamos National Laboratory, Los Alamos, NM 87545, USA*

[4]*National High Magnetic Field Laboratory and Department of Physics, Florida State University, Tallahassee FL 32310*

Pulsed magnetic fields of up to 55T are used to investigate the transport properties of the topological insulator $Bi_2Se_3$ in the extreme quantum limit. For samples with a bulk carrier density of n = $2.9 \times 10^{16}$cm$^{-3}$, the lowest Landau level of the bulk 3D Fermi surface is reached by a field of 4T. For fields well beyond this limit, Shubnikov-de Haas oscillations arising from quantization of the 2D surface state are observed, with the $\nu$ =1 Landau level attained by a field of $\sim$ 35T. These measurements reveal the presence of additional oscillations which occur at fields corresponding to simple rational fractions of the integer Landau indices.

The recent prediction and discovery that $Bi_2Se_3$ and $Bi_2Te_3$ are three-dimensional topological insulators (TI) [1–5] has sparked a flurry of investigations. In a magnetic field, their relativistic dispersion causes the energy spectrum to be quantized so that $E_\nu \propto \sqrt{B\nu}$, where $B$ is the magnetic field and $\nu = 1, 2, 3, ..$, is the energy level, known as the Landau level (LL). The progression of energy levels $E_\nu$ has been recently observed in scanning-tunneling microscopy (STM) on $Bi_2Se_3$[6, 7]. Other experiments on bulk samples and nanoribbons have reported universal conductance fluctuations attributed to the surface state[8, 9]. However, all of the unambiguous measurements for the existence of the surface state have been made by surface sensitive probes. In this letter, we study samples of $(Bi_{1-x}Sb_x)_2Se_3$ in which the Fermi surface of the Dirac fermions is small enough that pulsed fields of up to 55 T can access their quantum limit - the limit in which only a few of the lowest LLs are occupied. This is achieved by depleting the carrier density of the bulk and thereby reducing the size of the Dirac Fermi surface[10, 11]). We demonstrate for the first time, a system in which not only the *transport* properties of Dirac fermions can be studied, but studied in the 2D quantum limit where novel correlation effects are most likely to arise[12, 13].

Generally speaking, transport measurements in $Bi_2Se_3$ and $Bi_2Te_3$ are plagued by bulk conducting channels from either the conduction band or by impurity bands introduced by foreign dopants [14, 15]. The materials challenge is therefore finding a way to cleanly eliminate the bulk conductivity so that the properties of the surface can be observed. However, the carrier densities reported to date in studies of TI remain only as low[2–5] as $\sim 10^{18}$cm$^{-3}$. It has been known for some time that substituting isovalent Sb for Bi can reduce the size of the Fermi surface while retaining high mobilities [16]. By utilizing this idea and an optimized growth technique [11] we have reduced the bulk carrier density and corresponding Fermi surface systematically, while increasing the bulk resistivity by several orders of magnitude.

Crystals with bulk carrier densities of $2300 \times 10^{16}$cm$^{-3}$ and $33 \times 10^{16}$cm$^{-3}$ (red and orange curves on Figure 1 (a)) were obtained by slow cooling a binary melt with different Bi:Se ratio. The principal origin of these relatively high carrier densities is Se deficiency and antisite defects. Samples with n$\leq 11 \times 10^{16}$cm$^{-3}$ were obtained by slow cooling a ternary melt containing progressively more Sb. Although Sb is isovalent with Bi, Sb substitution apparently acts to control the defect density in the bulk crystals, reducing the bulk carrier density. Before measurements were performed, samples were cleaved on both sides with a scalpel blade in a dry atmosphere, mounted with contacts (using conductive silver epoxy) and pumped to $10^{-4}$mbar within 20 minutes. The leads made contact along the sides of the crystal to maximize the contact with the bulk. All samples were measured using a standard 4-probe configuration. Magnetoresistance and Hall effect measurements were performed at the National High Magnetic Field Laboratory (Los Alamos) in the short pulse ($\sim$10ms rise time) 55T magnet. Sweeps at both negative and positive field polarities were measured for all temperatures and angular positions. The data were then 'symmetrized' by combining the data from each field polarity to extract the components that are even in magnetic field (longitudinal magnetoresistance, $R_{xx}$) and odd in magnetic field (Hall resistance, $R_{xy}$).

In Figure 1 we illustrate the dependence of the resistivity on temperature for various samples with different carrier densities. The carrier density is determined by the (low field) Hall effect and can be matched to the size of the Fermi surface measured by quantum oscillations, which in resistivity are denoted Shubnikov-de Haas oscillations (SdHO) (see Figure 1 (b) to (d)). These oscillations are periodic in inverse field and their period $\Upsilon$ can be related to the extremal cross sectional area $A_k$ of the Fermi surface in momentum space via the Onsager relation $1/\Upsilon = (\hbar/2\pi e)A_k$. When the field is rotated about the crystal trigonal axis, the frequency of the SdHO

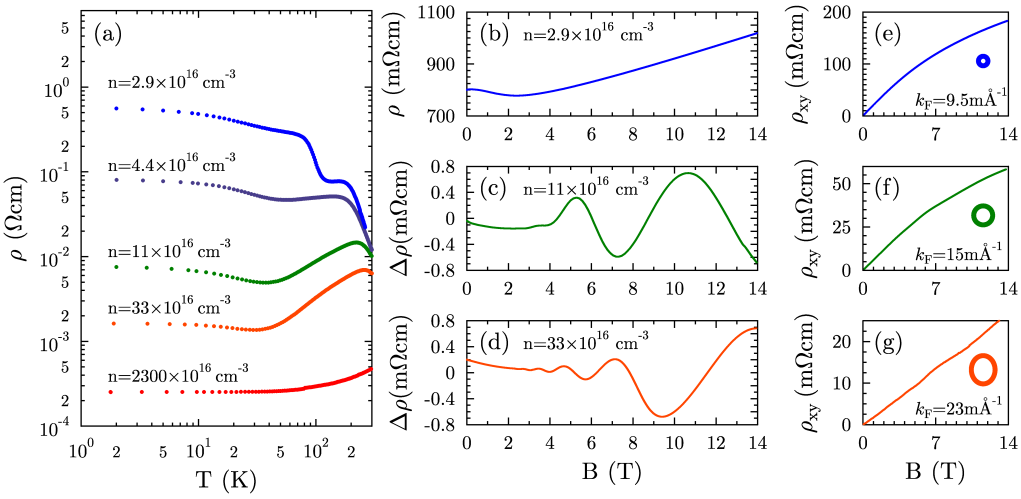


FIG. 1: (a) Progressively reducing the bulk carrier density in $Bi_2Se_3$ results in a significantly increased resistivity. A reduction in the carrier density from n=2300 $\times 10^{16}$cm$^{-3}$ to 33$\times 10^{16}$cm$^{-3}$ was achieved by varying the growth conditions for a binary melt. Further reduction in the bulk carrier density down to n= 2.9 $\times 10^{16}$ was achieved by isovalent substitution of Sb for Bi. (b-d) Representative magnetoresistance data at 2K for samples with indicated carrier densities, for field oriented along the trigonal c-axis. The progressive reduction of the Fermi surface volume is evident from the stretching of the SdH oscillations. (e-g) Carrier densities are extracted for each of these samples from the (low field) Hall effect. These are in very good agreement with those expected from the size of the Fermi surface (which shrinks monotonically as shown schematically in the lower right of each plot, with Fermi wavevector $k_F$ indicated). For the lowest carrier density samples shown in panels (e) and (f), the Hall signal deviates from linearity as the field approaches the 3D (bulk) quantum limit.

changes according to the morphology of the Fermi surface. In every one of our samples the bulk Fermi surface is a closed three-dimensional ellipsoid [11, 17, 18]. The effective mass $m^* \sim 0.12m_e$ varies weakly with doping for these carrier densities, as previously reported [17, 18]). For our lowest carrier density sample, the pocket is expected to have an orbitally averaged Fermi wavenumber of $k_F = 0.0095\mathring{A}^{-1}$. With such a small Fermi surface we are able to exceed the bulk 3D quantum limit with moderate fields $\sim 4T$. The remainder of this study is dedicated to the properties of the lowest carrier density samples at high fields.

In Figure 2 (a) we illustrate the symmetrized data for the longitudinal and transverse (Hall) resistances, $R_{xx}$ and $R_{xy}$ respectively, taken at 1.5 K on a sample (of carrier density n$\sim 3 \times 10^{16}$cm$^{-3}$) of dimensions $\sim$.63$\times$.36$\times$.15 mm$^3$. Strong features appear in the $R_{xy}$ and $R_{xx}$ signal at similar fields [19]. To investigate the dimensionality of the physics underlying these features, we rotate the crystal about the field, defining $\theta = 0$ to be when the field is perpendicular to the surface (parallel to the trigonal c-axis). For the 2D surface state of a topological insulator, quantum oscillatory phenomena depend only on the perpendicular component of the field $B_\perp$, and despite the peculiar Landau quantization $E_\nu$, the SdHO are still periodic in $1/B$[20]. In Figure 2 (b) and (c) we have plotted the $dR_{xy}/dB$ and $-d^2R_{xx}/dB^2$ as a function of $B_\perp = B\cos\theta$ - this would be the usual procedure to determine whether minima in the $R_{xx}$ (equivalent to minima in the negative second derivative) fall on top of the Hall plateaus (appearing as minima in the first derivative). Two pronounced dips in the Hall derivative are observed to correspond with the same dips in the magnetoresistance at all angles. The periodicity in $1/B$ of the minima indicates they arise from Landau quantization. In contrast to the angle dependence of the bulk Fermi surface of higher carrier density samples [11, 17, 18] these features scale with $1/\cos\theta$, providing unambiguous evidence that the plateau-like features in the Hall and minima in the SdHOs originate from a 2D metallic state.

Examining Figure 2 (b) the second and third minima occur at twice and three times the value in $1/B$ of the first, and it is natural to assign the indices $\nu = 1, 2, 3$ as shown. We plot these indices as a function of $1/B_\perp$ in Figure 3 (c) which connect a straight line through the origin. The plateau-like features in $R_{xy}$ are reminiscent of the quantum Hall effect in 2D electron gases [19, 20], but in the present case the quantization in integer multiples of $\sigma_0 = e^2/h$ is not evident[21]. This can be attributed to the presence of a large parallel conductance channel from the bulk. Nevertheless, this data conclusively shows that we are able to get to the quantum limit *of the 2D state.*

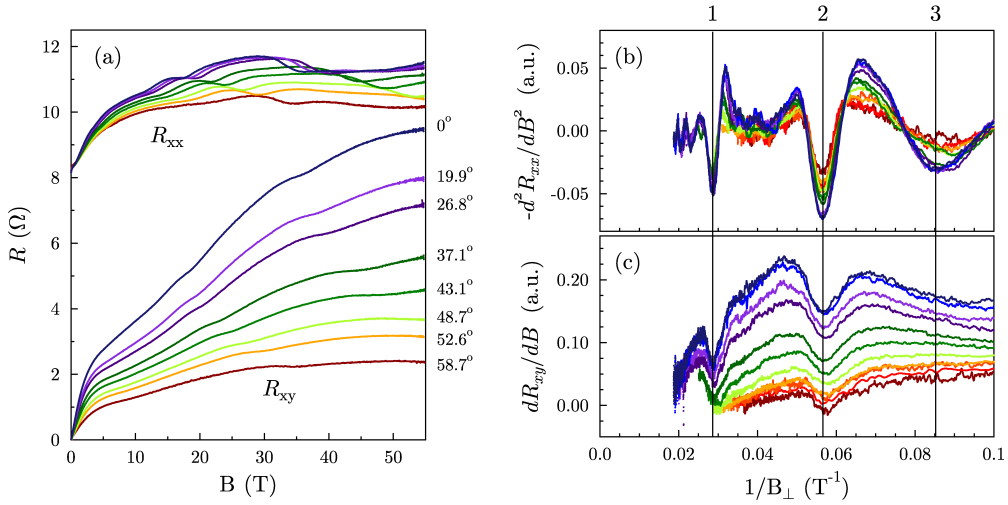


FIG. 2: (a) $R_{xx}$ and $R_{xy}$ data traces as a function of magnetic field for indicated angles for a single crystal with n$\sim 3\times10^{16}$cm$^{-3}$. The $R_{xx}$ traces are offset by +2.5 Ω. The deviation from linearity of the low-field $R_{xy}$ indicates the 3D quantum limit ($B \sim 4$T). Beyond this limit, additional features in both $R_{xy}$ and $R_{xx}$ move smoothly up in field as the tilt angle $\theta$ is increased. In contrast, the 3D quantum limit is independent of tilt angle. (b, c) $-d^2R_{xx}/dB^2$ and $dR_{xy}/dB$ as a function of $1/B_\perp$, where $B_\perp = B\cos\theta$ which aligns all features associated with the 2D surface state. The vertical lines are evenly spaced in $1/B_\perp$ and correspond to the filling of the first three energy levels $\nu$=1,2,3 of the 2D state.

The obvious candidate for the origin of the 2D states is the surface Dirac fermions.

A crude method to confirm that the effect is surface related is to briefly expose the sample to atmosphere. The atmosphere is a known $n$-type dopant of the surface[11] so that bulk carriers from the conduction band begin to contribute, smearing the surface signal. After 1-2 hours exposure the oscillatory phenomena we see in Figures 2 and 3 are almost completely absent(see Figure 4). We therefore conclude that the observed signal does indeed originate from the surface state of the TI. With this identification, we can determine the position of the Fermi energy on the Dirac cone from the period $\Upsilon$ of the oscillations. The Fermi wavevector $k_F$ of the surface state can be calculated from the Onsager relation above, yielding $k_F = 0.031\mathring{A}^{-1}$. Using the Fermi velocity measured by photoemission $v_F = 4.2\times10^5$ms$^{-1}$ [11], the Fermi energy is estimated to be ∼90meV above the Dirac point, or ∼110meV below the conduction band (see inset Figure 3 (c)).

It is important to distinguish this work from previous (unambiguous) measurements of the Dirac fermion, which have been mostly done in zero field[2–5]. The high magnetic field lifts the degeneracy of the Dirac cone at the Dirac point (defined in left inset Fig. 3 (c)) via the spin (Zeeman) coupling to the magnetic field, such that the quasiparticle gains a mass[25]. From the temperature dependence of the quantum oscillations we can estimate a cyclotron mass $m^* \propto dA_k/dE$ to be $0.11m_e$ for the surface fermions. It should be noted that even for a band with linear dispersion this value is finite and related to the Fermi velocity $v_F$ and the band filling[26]. In the present case $v_F = 4.2\times10^5$ms$^{-1}$ and $E_F = 90$meV (see below) would give $m^* = 0.089m_e$. The difference with the measured mass provides a measure of the band curvature of the split bands. This splitting fundamentally changes the topology of the Dirac cone. In an unsplit system, like graphene, the crossing at the Dirac point gives a Berry's phase factor which results in a finite index intercept at 1/2[26, 27].When the Dirac cone is split (the fermions are massive[25]), this Berry's phase should not exist, suggesting that the plot of $\nu$ vs $1/B$ extrapolates to $(0,0)$[27], as is presently observed (see Figure 3 (c)). Our data is therefore consistent with the observation of this surface state with a split Dirac cone.

In Figure 3 (a) and (b) we plot $-d^2R_{xx}/dB^2$ vs $1/B_\perp$ in the range $0 < \nu < 1$ and $1 < \nu < 2$ respectively. Minima in the signal emerge at each angle which line up when plotted as a function of $1/B_\perp$, and therefore also evidence 2D physics. These minima are not periodic in inverse field and cannot originate from another Fermi surface. They are also reproducible using different sweep rates of the pulsed magnetic field and thus cannot be artifacts of the pulsed magnet environment that are periodic in time. Intriguingly, these minima fall very near simple rational fractions of 2/3, 5/7 and 4/5 (in Fig. 3 (a) as well as 6/5, 4/3, 3/2 and 5/3 (in Fig. 3(b)).

Aperiodic 'oscillations' are typical of quantum interference phenomena in mesoscopic systems, and we cannot rule out the possibility that this is the origin of the addi-

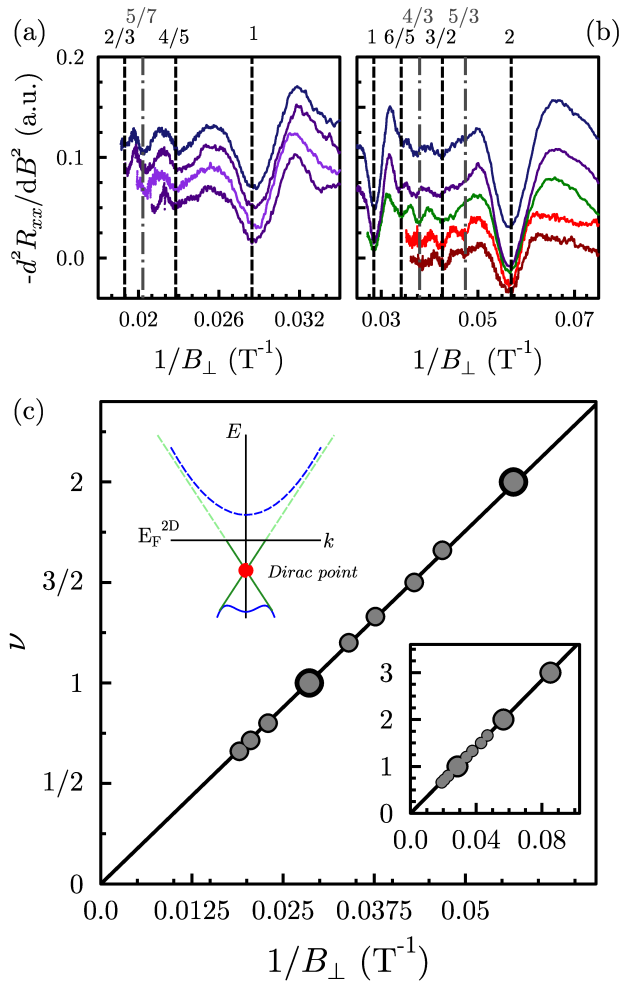


FIG. 3: (a) $-d^2R_{xx}/dB^2$ as a function of $1/B_\perp$ in the field range for which $\nu < 1$ for $\theta = 0°$, $9.1°$, $19.9°$ and $26.8°$ (top to bottom), illustrating three additional features at fields corresponding to fractional landau indices. (b) The same signal for the field range for which $1 < \nu < 2$ for angles $\theta = 0°$, $19.9°$, $43.1°$, $55.7°$, $58.7°$, illustrating four further features. These additional oscillations scale with the the perpendicular component of the field to the surface just as in Figure 2, illustrating that they must also originate from the 2D surface state. Assigning indices for these features based on the integer indices gives values of $\nu = 0.665\pm0.005, 0.72\pm0.01, 0.805\pm0.005$ for $\nu < 1$ and $1.19 \pm 0.02, 1.32 \pm 0.02, 1.51 \pm 0.03, 1.65 \pm 0.03$ for $1 < \nu < 2$, (counting from small to large $1/B$). Vertical lines are drawn in panels (a) and (b) corresponding to the nearest fractional Landau filling. (c) LL index $\nu$ as a function of inverse field. Large symbols show integer levels $\nu = 1, 2, 3$. Small symbols show fractional features observed in panels (a) and (b). The data are fit by straight line. The period of the integer states gives an estimate of the surface state $E_f$, which would cross 90 meV above the Dirac point corresponding to 110meV below the conduction band as shown in the schematic (upper left inset) [11].

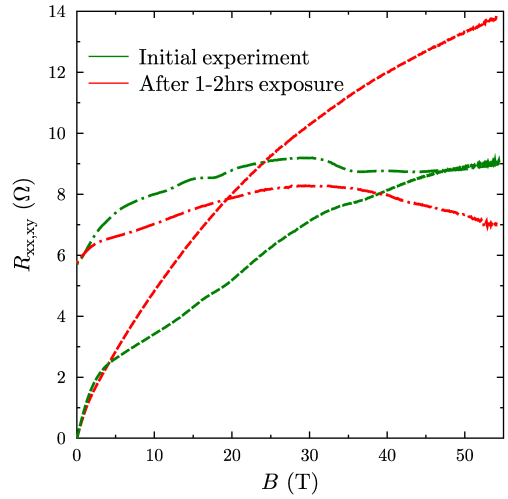


FIG. 4: The $R_{xx}$ (dash-dot line) and $R_{xy}$ (dashed line) signal shown in green before exposure shows the oscillations related to the 2D state. The red curves show the signal after this sample is exposed to atmosphere for 1-2 hours, with greatly suppressed oscillatory signal in $R_{xx}$, and no apparent signature in $R_{xy}$.

tional non-periodic features seen in Fig 3 (a) and (b)[9]. However, the correspondence of these minima to simple fractions of the integer Landau indices is striking, suggesting that they might be precursors of the fractional QHE. The relatively low bulk mobility in the present samples ($\sim$400cm$^2$/Vs) argues against such an interpretation, but on the other hand, it is not clear whether the mobility of the surface state is actually higher than that of the bulk. It is instructive to note that the integer QHE in graphene was seen for samples with mobilities around 40 times the present (bulk) mobility[26]. The distinct steps presently observed in $R_{xy}$ at integer Landau indices (reminiscent of the integer QHE) argues for a higher surface mobility.

Except for the fraction 3/2, the observed fractions indicated in Fig.3 are where the classic *fractional* quantum Hall effect (QHE) would be expected to be most robust. In semiconductors, the strongest even denominator fraction occurs at 5/2, a state that is both much weaker than odd-denominator fractions[22] and is unusual in that it is a spin-unpolarized FQH state [23]. We note that the data in Fig. 3(b) show the even denominator and odd denominator fractions to be of similar strength. If these features are ascribed to the FQHE, this suggests that the strong spin-orbit coupling in a TI may enable the Dirac quasiparticles to condense into both symmetric and antisymmetric Laughlin wavefunctions[24].

By suppressing the bulk carrier density in $(Bi_{1-x}Sb_x)_2Se_3$ we have demonstrated that the transport properties of the metallic surface state of this topological insulator can be investigated in the

quantum limit. The application of high magnetic fields reveals quantum oscillations arising from this new two-dimensional system, including features at fields corresponding to *fractional* values of the integer Landau indices. As such, experimental access to the surface state of $(Bi_{1-x}Sb_x)_2Se_3$ provides a new laboratory for studying topological quantum matter and potentially correlations among Dirac fermions [12, 13].

The authors would like to thank Oscar Vafek, David Goldhaber-Gordon, Jimmy Williams, Shoucheng Zhang, Xiaoliang Qi, Chao-xing Liu, Joseph Maciejko, Yulin Chen, and Joel Moore for useful discussions. The NHMFL is supported by NSF Division of Materials Research through DMR-0654118. RMcD acknowledges support from the U.S. DOE, Office of Basic Energy Sciences 'Science in 100 T' program. This work is supported by the Department of Energy, Office of Basic Energy Sciences under contract DE-AC02-76SF00515.

[1] H. Zhang, *et al.*, Nat Phys **5**, 438 (2009), ISSN 1745-2473.
[2] Y. L. Chen, *et al.*, Science **325**, 178 (2009).
[3] D. Hsieh, *et al.*, Nature **460**, 1101 (2009), ISSN 0028-0836.
[4] D. Hsieh, *et al.*, Science **323**, 919 (2009).
[5] Z. Alpichshev, *et al.*, Physical Review Letters **104**, 016401 (2010).
[6] P. Cheng, *et al.*, 1001.3220 (2010).
[7] T. Hanaguri, K. Igarashi, M. Kawamura, H. Takagi, and T. Sasagawa, 1003.0100 (2010).
[8] H. Peng, *et al.*, Nat Mater **9**, 225 (2010), ISSN 1476-1122.
[9] J. G. Checkelsky, *et al.*, Physical Review Letters **103**, 246601 (2009).
[10] L. Wray, *et al.*, 0912.3341 (2009).
[11] J. G. Analytis, *et al.*, 1001.4050 (2010).
[12] Y. Ran, H. Yao, and A. Vishwanath, 1003.0901 (2010).
[13] M. Levin and A. Stern, Physical Review Letters **103**, 196803 (2009).
[14] J. Kasparova, *et al.*, Journal of Applied Physics **97**, 103720 (2005).
[15] M. K. Zhitinskaya, S. A. Nemov, T. E. Svechnikova, and E. Mller, Semiconductors **38**, 182 (2004).
[16] V. A. Kulbachinskii, *et al.*, Physical Review B **59**, 15733 (1999).
[17] H. Kohler and A. Fabbicius, physica status solidi (b) **71**, 487 (1975).
[18] H. Kohler, Physica Status Solidi (b) **58**, 91 (1973).
[19] S. D. Sarma and A. Pinczuk, *Perspectives in Quantum Hall Effects: Novel Quantum Liquids in Low-Dimensional Semiconductor Structures* (Wiley-Interscience, 1996), ISBN 047111216X.
[20] K. S. Novoselov, *et al.*, Science **315**, 1379 (2007).
[21] L. Fu and C. L. Kane, Physical Review B **76**, 045302 (2007).
[22] R. Willett, *et al.*, Physical Review Letters **59**, 1776 (1987).
[23] J. P. Eisenstein, *et al.*, Physical Review Letters **61**, 997 (1988).
[24] R. B. Laughlin, Physical Review Letters **50**, 1395 (1983).
[25] S. Shen, 0909.4125 (2009).
[26] K. S. Novoselov, *et al.*, Nature **438**, 197 (2005), ISSN 0028-0836.
[27] G. P. Mikitik and Y. V. Sharlai, Physical Review Letters **82**, 2147 (1999).